

● *Contributed Paper***DEPHASING OF HAHN ECHO IN ROCKS BY DIFFUSION IN SUSCEPTIBILITY-INDUCED FIELD INHOMOGENEITIES**

M.D. HÜRLIMANN,* K.G. HELMER,*† AND C.H. SOTAK†‡

*Schlumberger-Doll Research, Ridgefield, CT; †Department of Biomedical Engineering, WPI, Worcester, MA; and ‡Department of Radiology, University of Massachusetts Medical School, Worcester, MA, USA

The decay of the Hahn spin echo of water in the pore space of many porous media is dominated by the dephasing of spins in internal-field inhomogeneities, produced by susceptibility contrasts, rather than surface or bulk relaxation. This is particularly the case for measurements at moderate and high fields in samples such as fluid-saturated sedimentary rocks and some biological materials. Here, we study the behavior of the Hahn-echo decay in rocks with grains much larger and smaller than the average dephasing length, which is typically of the order of a few microns. It is shown that the decay in these two cases is qualitatively different. For coarse-grained rocks, the decay can be modeled to first order by a distribution of local, effective field gradients. This is in contrast to the case of fine-grained rocks, where motional narrowing of the field inhomogeneities occurs. These interpretations are supported by measurements of the temperature dependence of the Hahn echo decay and the diffusion time dependence of the diffusion coefficient. © 1998 Elsevier Science Inc.

Keywords: NMR relaxation; Restricted diffusion; Sedimentary rocks.

INTRODUCTION

Nuclear magnetic resonance measurements have become an important tool to characterize fluid-saturated porous media, such as biological samples or sedimentary rocks. In these samples, there is often a significant susceptibility contrast, $\Delta\chi$, between the solid material and the fluid filling the pore space. In many cases, the decay of the Hahn spin echo is dominated by diffusion of the spins in the resulting field inhomogeneities, rather than relaxation on surfaces or in the bulk liquid. This is clearly the case for sedimentary rocks at high fields,^{1,2,3,4,5} and similar situations exist in some biological samples when air bubbles, red blood cells or magnetic contrast agents produce field inhomogeneities.^{6,7}

The dephasing of the Hahn spin echo, at a total echo time 2τ , due to diffusion in the inhomogeneous field, $B_0(r)$, depends on the path integral $I(\tau)$ of the instantaneous Larmor frequency, $\omega(t) \equiv \gamma B_0(r(t))$:

$$I(\tau) = \left\langle \exp \left\{ i \int_0^\tau \omega(t) dt - i \int_\tau^{2\tau} \omega(t) dt \right\} \right\rangle. \quad (1)$$

Here the average is evaluated over all spins. In order to evaluate this expression, both the spatial distribution of the static magnetic field in the pore space, $B_0(r)$, and the properties of restricted diffusion, i.e., $r(t)$, have to be known accurately. Detailed, realistic information on the pore geometry and the field distribution in a sedimentary rock is usually not available. For this reason we first identify the critical features of the pore geometry and field profile needed to capture the essential physics of the problem. These elements are then used to describe the complicated processes in a simplified manner. To highlight these underlying features, we first summarize the behavior of the resultant Hahn echo with the addition of a field gradient in simple restricting geometries and then

Address correspondence to Dr. Martin Hürlimann, Schlumberger-Doll Research, Ridgefield, CT 06877-4108, USA

discuss some generalizations to more complicated systems. We compare this simplified description with experimental results, including the temperature dependence of the Hahn echo and the diffusion-time dependence of the diffusion coefficient.

RESTRICTED DIFFUSION IN A NON-UNIFORM FIELD

In simple geometries characterized by a single-length scale, it has been shown^{8,9,10} that the decay of the Hahn echo for spins diffusing in an applied gradient g is governed by the interplay of three lengths: the diffusion length, $l_D \equiv \sqrt{D_0\tau}$, (D_0 is the self-diffusion coefficient), the size of the pore or structure, l_s , and a dephasing length, $l_g \equiv (D_0/\gamma g)^{1/3}$, (γ is the gyromagnetic ratio). The diffusion length gives a measure of the average distance that a spin diffuses during the time τ . The dephasing length l_g may be thought of as the typical length scale over which a spin must travel to dephase by 2π radians. For gradients in the range of 1 to 1000 G/cm and the diffusion coefficient of water at room temperature, l_g varies between about 10 μm and 1 μm .

At short enough diffusion times l_D is the shortest length. In this free-diffusion regime, the echo decays approximately as:¹¹

$$M(g, \tau)/M_0 = \exp \left\{ -\frac{2}{3} D_0 \gamma^2 g^2 \tau^3 \right\}, \quad (2)$$

where M_0 is the signal amplitude at zero gradient strength.

At longer diffusion times when l_D becomes larger than l_s or l_g , the behavior depends on the ratio l_s/l_g . When this ratio is small compared to 1, (i.e., in small pores where l_s becomes the shortest length), the spins average out the field inhomogeneities. In the motional averaging regime, the echo amplitude for $\tau \gg l_s^2/D_0$ decays asymptotically as:¹²

$$M(g, \tau)/M_0 = \exp \left\{ -\frac{8}{175} \frac{\gamma^2 g^2 l_s^4 2\tau}{D_0} \right\}. \quad (3)$$

Eq. (3) is appropriate for spherical pores. For other geometries, Neuman¹² showed that only the numerical prefactor in the exponent changes.

In the other case in which $l_s/l_g \gg 1$, the decay of the spin echo start to deviate significantly from Eq. (2) only after it has decayed to a low level, that scales like l_g/l_s , and eventually reaches what we have called the localization regime.¹⁰

The above discussion can be generalized to more complicated situations, such as sedimentary rocks, in the

following way. In these disordered systems, the field variations are more complicated than can be described by a single gradient, and the restrictions are, in general, more diverse and cannot be described by a single-length scale. However, for any small subset of spins, it is still useful to identify the dominant regime for the Hahn echo decay (free diffusion, motional averaging, or localization regime). In the free-diffusion regime, appropriate for coarse-grained rocks, the majority of the spins' signal decays before they have experienced significant restrictions due to the grains. At longer times, the echo decay will show a localization-type behavior. In the motional averaging regime, appropriate for fine-grained rocks, the spins are severely restricted before their signal has decayed. The distinction between fine- and coarse-grained rocks is given by the relative size of a representative dephasing length, l_g , and a typical length scale for the restriction, l_s . This separation corresponds to the separation between "small size" and "large size" discussed by Muller et al.⁶

In the free-diffusion regime, the typical pore size is large enough that the echo amplitude decays before a significant fraction of the spins have experienced the effect of the walls. For this purpose, the diffusion of the spins is then, essentially, free. Each spin will experience some local, effective gradient g_{eff} . The effective gradient g_{eff} is equal to the local gradient, g , averaged over the length l_g . This length has to be determined self-consistently by $l_g = (D_0/\gamma g_{eff})^{1/3}$ and is typically in the range of a few microns. Field inhomogeneities on a length scale shorter than l_g are not important because they are averaged out by diffusion. The expected echo decay is then to first order a superposition for spins with the appropriate g_{eff} :

$$M(\tau)/M_0 \approx \int f(g_{eff}) \exp \left\{ -\frac{2}{3} D_0 \gamma^2 g_{eff}^2 \tau^3 \right\} dg_{eff}, \quad (4)$$

where $f(g_{eff})$ is the distribution of effective gradients in the rock. We stress that this expression will only be approximately correct, as further discussed in Refs. 10 and 13. For rocks in the free diffusion regime, we can try to invert the measured Hahn echo decay and obtain a rough distribution of effective gradients. The width of the distribution is due to the gradient distribution within a pore and due to the heterogeneity between different pores.

For a fine-grained rock, we expect that the echo follows Eq. (4) only for a short time. After the spins have diffused across the pore, the echo decay will be at a reduced rate and similar to Eq. (3). This equation was derived for diffusion in a bounded space and in the presence of an applied constant gradient. Following the

argument of Wayne and Cotts,¹⁴ a similar behavior will also apply for diffusion in an unbounded space but with a bounded field variation. Note that in Eq. (3), gl_s is the total field variation that the spins are exposed to. In our case, this quantity will scale like $\Delta\chi B_0$.⁴ The important correlation time of the field fluctuations that the spins experience is given by $\tau_c = l_s^2/D_{eff}$, where D_{eff} is the long time diffusion coefficient, i.e., D_0 divided by the tortuosity \mathcal{T} .¹³ The tortuosity limit is approached after a diffusing spin has sampled a large enough part of the pore space to be representative of the whole pore space. The expected decay is then given by:

$$M(\tau)/M_0 \approx \exp \left\{ -\alpha (\gamma \Delta\chi B_0)^2 \frac{l_s^2}{D_{eff}} \tau \right\}. \quad (5)$$

Here, we use α to indicate a factor that depends on the exact shape of the pores, similar to the situation discussed in Ref. 12 concerning Eq. (3).

RESULTS AND DISCUSSION

NMR measurements were compared between two rocks with very different pore sizes. The goal was to find rocks where the pore size is either much larger or much smaller than the dephasing length l_g . The first rock is a coarse-grained sandstone, a quarried sample of Fontainebleau sandstone, consisting of clean sand grains with an average grain size of about 200 μm , a porosity of 9.2%, a tortuosity $\mathcal{T} = 4.9$ and a susceptibility contrast to water of $\Delta\chi = +2.11 \times 10^{-6}$ (SI). The second rock is a fine-grained carbonate made up of small micrite particles of size $\leq 2 \mu\text{m}$. This mudstone has a porosity of 22.7%, a tortuosity $\mathcal{T} = 2.8$ and a susceptibility contrast to water of $\Delta\chi = +1.22 \times 10^{-6}$ (SI). Both rock cores were cylindrical plugs with diameters of 2 cm and lengths of 3.8 cm. They were fully saturated by vacuum impregnation with a brine solution of conductivity $\sigma_w = 5$ S/m.

The measurements were performed with a GE 2.0 T CSI-II imaging spectrometer, operated at a Larmor frequency of 85.56 MHz and equipped with self-shielded gradients able to achieve a maximum gradient strength of ± 20 G/cm. Measurements were performed at temperatures of $T = 25^\circ\text{C}$ and 40°C .

In Fig. 1a and b, we show the measured Hahn echo decay at the two temperatures for the sandstone and the carbonate rocks, respectively. It is evident that for the sandstone, the decay rate increases as the temperature is increased, whereas for the fine-grained rock, we observe the opposite behavior. Similar behavior has been observed by Weisskoff et al.⁷ for samples of monosized beads. This is indeed what is expected from Eqs. (4) and (5), respectively. By raising the temperature from 25.0°C to 40°C , the diffusion coefficient is increased by 40%. As

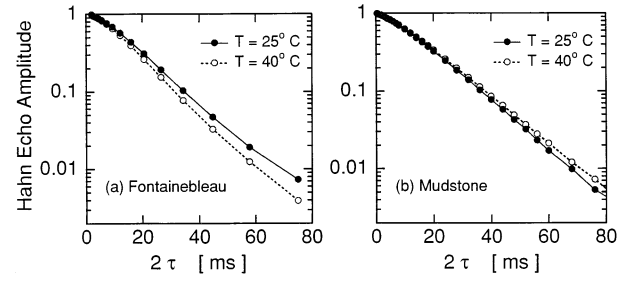


Fig. 1. Decay of Hahn-echo amplitude versus the total echo spacing, 2τ , for the Fontainebleau sandstone (a) and a carbonate mudstone (b) at two temperatures. The lines connecting the data points are drawn only to guide the eye.

the temperature is raised, diffusion is more rapid, which leads to greater decay in the free-diffusion regime, and to a better averaging and smaller decay in the motional-averaging regime.

In the case of the sandstone, the temperature dependence agrees quantitatively with the simple expression (4). To show this clearly, we replot in Fig. 2 the sandstone data of Fig. 1a as echo amplitude versus $(\gamma^2 D_0 \tau^3)^{1/3}$. The data of the two temperatures now fall on the same curve. This confirms that spins are essentially in the free-diffusion limit and that the pore size is larger than the individual dephasing lengths. The high degree of collapse seen in Fig. 2 may be partly fortuitous, however, considering the limitations to Eq. (4) mentioned above.

We have further NMR evidence that the typical pore size in the sandstone is larger than a few microns. In Fig.

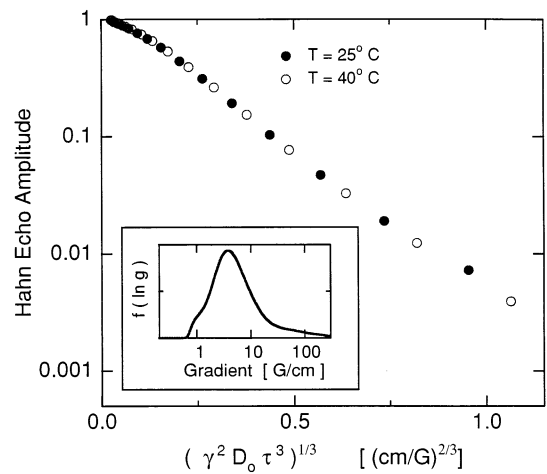


Fig. 2. Decay of Hahn echo amplitude versus the rescaled echo spacing, $(\gamma^2 D_0 \tau^3)^{1/3}$, for the Fontainebleau sandstone at two temperatures. The data overlap implies that Eq. (4) is generally followed. The distribution of effective gradients obtained by an analysis of this data is shown in the insert.

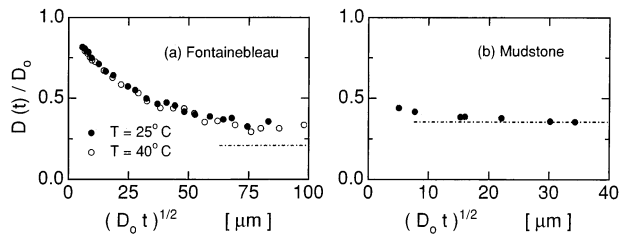


Fig. 3. Time-dependent diffusion coefficient, $D(t)$, versus the diffusion length, l_D , for the Fontainebleau sandstone (a) at $T = 25^\circ\text{C}$ and $T = 40^\circ\text{C}$ and carbonate mudstone (b) at $T = 25^\circ\text{C}$. The dashed-dotted line shows the tortuosity limit, determined independently by electrical measurements.

3, the measured values of the time-dependent diffusion coefficient, $D(t)$, normalized with respect to D_0 are displayed for both samples. The measurements were obtained with a sequence that uses pulsed, bipolar gradients and is based on the stimulated echo.¹⁵ The data has been analyzed as described in detail in 16. The sandstone data in Fig. 3a shows that the measured diffusion coefficient is decreasing relatively slowly from D_0 towards the tortuosity limit, $D_{eff} = D_0/\mathcal{T}$, shown as dash-dotted line. The tortuosity \mathcal{T} has been determined independently by electrical measurements. The Hahn echo has decayed to e^{-1} at an echo time of about 18 ms. This corresponds to a diffusion length $l_D \approx 6 \mu\text{m}$. For this diffusion length, the measured diffusion coefficient is much closer to D_0 than D_{eff} . This further confirms that the typical pore size of this coarse-grained rock is larger than the dephasing length and, therefore, that the free-diffusion regime is indeed appropriate to describe the Hahn echo decay to first order. Even at the longest echo spacing shown in Fig. 1a, the spins have diffused less than $16 \mu\text{m}$ and the measured diffusion coefficient is still far from the tortuosity limit D_{eff} .

In the case of the mudstone shown in Fig. 1b, the slower decay at higher temperature is qualitatively in agreement with Eq. (3). Faster diffusion leads to increased averaging of the field inhomogeneities and leads to a reduced decay rate. Brown and Fantazzini⁴ have observed similar behavior in fine-grained porcelain samples. The decrease, however, is weaker than predicted from the asymptotic expression in Eq. (3) and the temperature dependence of the diffusion coefficient. The simplest explanation is that $l_s \ll l_g$ is not strictly fulfilled, i.e., the typical pore size of $1 \mu\text{m}$ is smaller than the dephasing length, but not by a large factor. The observed temperature dependence might also be affected by a few larger pores. This has been confirmed by analysis of electron microscopy thin sections. The data in Fig. 3b shows the time-dependent diffusion coefficient for the mudstone. These measurements approach the tortuosity limit much faster than in Fig. 3a, and coincide

with the tortuosity limit at the longer diffusion lengths. This indicates that spins have diffused through several pores and that the pore size in the mudstone is indeed much smaller than in the sandstone. Note that at the shorter diffusion lengths shown in Fig. 3b, the measured diffusion coefficient deviates somewhat from the tortuosity limit. This also demonstrates that the tail of the pore-size distribution extends to some larger pores.

The temperature dependence of the echo decay for the coarse grained sandstone, shown in Figs. 1a and 2, supports the description by Eq. (4). To first order, each spin is exposed to a local effective gradient, g_{eff} , and there is a distribution $f(g_{eff})$ of these gradients in the pore space of the rock. The actual gradients are, of course, not uniform. For Eq. (4) to be applicable, however, they only need to be constant over the distance l_g , i.e., a few microns. Taking this expression at face value, we can extract the distribution of the effective gradients, $f(g_{eff})$ from the data shown in Fig. 1a. The resulting distribution, calculated using a procedure implemented by A. Sezginer and described in Ref. 17, is shown in the insert of Fig. 2. Note that while the mode of the distribution is centered around 4 G/cm, the distribution has a significant high-gradient tail that extends to over 100 G/cm. This shows that, even in samples with fairly uniform grain sizes, the distribution of gradients can be substantial and some spins will experience rapid dephasing in the pores corresponding to the high-gradient tails of the distribution. In separate diffusion-edited T_1 measurements, we have confirmed that spins in the smaller pores experience the highest effective gradients.

The maximum of the distribution at approximately 4 G/cm agrees with an order of magnitude estimate: we expect that the mean gradient is of order $\Delta\chi B_0/2l_{pore}$.² In this rough estimate, a 4-G/cm gradient corresponds to a pore size of about $50 \mu\text{m}$, which is consistent with a grain size of $200 \mu\text{m}$.

In the case of the mudstone, the temperature dependence gives an indication of motional averaging. We can also make an order of magnitude estimate to confirm that this interpretation is reasonable. At the longer times, the Hahn echo decays with a decay rate of approximately $(13.5 \text{ ms})^{-1}$. Using Eq. (3), estimating $gl_s \approx \Delta\chi B_0$ and using the long time limit for the diffusion coefficient, we obtain $l_s \approx 1.8 \mu\text{m}$, a number close to the size of the micrite particles that make up this rock.

CONCLUSIONS

In conclusion, we have investigated the effects of internal-field gradients in two rock cores using the decay of the Hahn echo and the diffusion-time dependence of the water diffusion coefficient. Samples were chosen with differing characteristic pore sizes. The first sample

was a large-grained sandstone in which the echo decay can be represented as free diffusion in an effective gradient field. In this case, the distribution of effective gradients can be extracted by inverting the Hahn echo data. The second, fine-grained sample, a mudstone, had less decay as the diffusion coefficient of the pore-filling fluid was raised. This signalled that the spins were experiencing motional narrowing of the field inhomogeneities.

Acknowledgments—We thank P. Sen, R. Kleinberg, and T. de Swiet for useful discussions and W. Kenyon and D. Rossini for the electron microscopy images.

REFERENCES

1. Bendel, P. Spin-echo attenuation by diffusion in nonuniform field gradients. *J. Magn. Reson.* 86:509–515; 1990.
2. Kleinberg, R.L.; Horsfield, M.A. Transverse relaxation processes in porous sedimentary rock. *J. Magn. Reson.* 88:9–19; 1990.
3. Borgia, G.C.; Brown, R.J.S.; Fantazzini, P.; Mesini, E.; Valdré, G. Diffusion-weighted spatial information from ^1H Relaxation in restricted geometries. *Il Nuovo Cimento* 14 D:745–752; 1992.
4. Brown, R.J.S.; Fantazzini, P. Conditions for initial quasi-linear T_2^{-1} versus τ for Carr-Purcell-Meiboom-Gill NMR with diffusion and susceptibility differences in porous media and tissues. *Phys. Rev. B* 47:14823–14834; 1993.
5. Borgia, G.C.; Brown, R.J.S.; Fantazzini, P. Scaling of spin-echo amplitudes with frequency, diffusion coefficient, pore size, and susceptibility difference for the NMR of fluids in porous media and biological tissues. *Phys. Rev. E* 51:2104–2114; 1995.
6. Muller, R.N.; Gillis, P.; Moyny, F.; Roch, A. Transverse relaxivity of particulate MRI contrast media: From theories to experiments. *Magn. Reson. Med.* 22:178–182; 1991.
7. Weisskoff, R.M.; Zuo, C.S.; Boxerman, J.L.; Rosen, B.R. Microscopic susceptibility variation and transverse relaxation: theory and experiment. *Magn. Reson. Med.* 31:601–610; 1994.
8. Stoller, S.D.; Happer, W.; Dyson, F.J. Transverse spin relaxation in inhomogeneous magnetic fields. *Phys. Rev. A* 44:7459–7477; 1991.
9. de Swiet, T.M.; Sen, P.N. Decay of nuclear magnetization by bounded diffusion in a constant field gradient. *J. Chem. Phys.* 100:5597–5604; 1994.
10. Hürlimann, M.D.; Helmer, K.G.; de Swiet, T.M.; Sen, P.N.; Sotak, C.H. Spin echoes in a constant gradient and in the presence of simple restriction. *J. Magn. Reson. A* 113:260–264; 1995.
11. Hahn, E.L. Spin echoes. *Phys. Rev.* 80:580–594; 1950.
12. Neuman, C.H. Spin echo of spins diffusing in a bounded medium. *J. Chem. Phys.* 60:4508–4511; 1974.
13. Helmer, K.G.; Hürlimann, M.D.; de Swiet, T.M.; Sen, P.N.; Sotak, C.H. Determination of ratio of surface area to pore volume from restricted diffusion in a constant field gradient. *J. Magn. Reson. A* 115:257–259; 1995.
14. Wayne, R.C.; Cotts, R.M. Nuclear-magnetic-resonance study of self-diffusion in a bounded medium. *Phys. Rev.* 151:264–272; 1966.
15. Latour, L.L.; Li, L.; Sotak, C.H. Improved PFG stimulated-echo method for the measurement of diffusion in inhomogeneous fields. *J. Magn. Reson. B* 101:72–77; 1993.
16. Hürlimann, M.D.; Helmer, K.G.; Latour, L.L.; Sotak, C.H. Restricted diffusion in sedimentary rocks: Determination of surface-area to volume ratio and surface relaxivity. *J. Magn. Reson. A* 111:169–178; 1994.
17. Fordham, E.J.; Sezginer, A.; Hall, L.D. Imaging multiexponential relaxation in the $(y, \log_e T_1)$ plane, with application to clay filtration in rock cores. *J. Magn. Reson. A* 113:139–150; 1995.